

Optimized Sampling Strategies for Isoniazid in East Asian Pediatric Populations Using Population Pharmacokinetics-Informed Approaches

Gegang Ju¹⁻³, Xin Liu⁴, Yeheng Peng⁴, Wenyu Yang⁴, Nuo Xu⁴, Qingfeng He⁴, Chenchen Zhang⁵, Lulu Chen^{3,6}, Nan Yang^{3,6,7}, Gufen Zhang^{3,6,7}, Chao Li^{3,6,7}, Pan Su⁸, Xiao Zhu⁴, Dongsheng Ouyang^{1-3,6}

¹Department of Clinical Pharmacology, Xiangya Hospital, Central South University, Changsha, People's Republic of China; ²Institute of Clinical Pharmacology, Central South University, Changsha, People's Republic of China; ³Hunan Key Laboratory for Bioanalysis of Complex Matrix Samples, Changsha Duxact Biotech Co., Ltd., Changsha, People's Republic of China; ⁴Department of Clinical Pharmacy, School of Pharmacy, Fudan University, Shanghai, People's Republic of China; ⁵School of Pharmaceutical Sciences, Sun Yat-Sen University, Guangzhou, People's Republic of China; ⁶Changsha Duxact Biotech Co., Ltd., Changsha, People's Republic of China; ⁷Phamark Data Technology Co., Ltd., Changsha, People's Republic of China; ⁸Hunan Chest Hospital, Changsha, People's Republic of China

Correspondence: Dongsheng Ouyang, Department of Clinical Pharmacology, Xiangya Hospital, Central South University, Lutian Road 28, Changsha, People's Republic of China, Tel +86 0731 84805380, Email 801940@csu.edu.cn; Xiao Zhu, Department of Clinical Pharmacy, School of Pharmacy, Fudan University, Jinke Road 3728, Shanghai, People's Republic of China, Tel +86 21 51980025, Email xiaozhu@fudan.edu.cn

Objective: Isoniazid exposure in vivo is significantly affected by NAT2 genotypes and has ethnic differences. To optimize the sampling strategy for isoniazid in East Asian pediatric populations. We employed a model-informed optimization approach based on INH population pharmacokinetic (PopPK) models.

Methods: We selected PopPK models for children and East Asian adults and optimized the sampling strategy using PopED (Population Experimental Design), a method that helps identify the most efficient sampling points for maximizing parameter estimation accuracy. Virtual patients with varying NAT2 phenotypes were created, and real-world pediatric scenarios were evaluated using questionnaire data, sampling windows, and stochastic simulations.

Results: From eight analyzed models (four for East Asian adults and four for non-East Asian pediatrics), we simplified two over-parameterized models using lumping without loss of performance. The optimized clinical sampling strategy involved collecting samples at 0.25 [0–0.5], 1.5 [1–2], 6 [3–8], 12 [9–14], and 24 [22–24] hours post-dose. Simulation verification showed that re-estimated major PK parameters had acceptable relative biases and relative standard error (<30%).

Conclusion: Traditional adult sampling strategies are inadequate for East Asian pediatric populations. A tailored strategy involving up to five samples can accurately estimate INH PopPK parameters and should be considered for clinical implementation to optimize treatment and reduce patient sampling burden.

Keywords: isoniazid, optimal sampling design, population pharmacokinetics, stochastic simulation and estimation

Introduction

Tuberculosis (TB) is a highly infectious disease that ranks as the second leading cause of death worldwide, following COVID-19, according to the latest report by the World Health Organization (WHO) on global tuberculosis, and East Asia, Africa, and India are still classified as high-burden tuberculosis (TB) countries or regions.¹ To combat TB, typically requires multidrug therapy, isoniazid (INH) stands out as the most critical first-line drug and is widely used for both the prevention and treatment of TB in adult and pediatric patients.² Despite the significant advancements made in anti-TB drugs, there is still a considerable percentage of patients (more than 14%) who fail to respond to treatment. One of the major reasons for this is suboptimal exposure to anti-TB drugs.³

In the case of INH, which is considered the most important first-line drug against TB, its efficacy relies heavily on its absorption rate in the human body.² Fortunately, INH is rapidly and completely absorbed in humans (>90%) when taken orally. Once absorbed, INH distributes extensively throughout the body, including body fluids and tissues such as the cerebrospinal fluid and pleural fluid. Another advantage is that INH has a low binding rate with plasma proteins, ranging from 0% to 10%.⁴ This allows for better distribution and efficacy of the drug. To optimize the administration of INH, the WHO has developed consolidated guidelines that recommend different dosages based on age and body weight. For individuals aged 10 years and older, the normal daily dose is 300 mg, with a range of 4–5mg/kg. For those younger (<10 years) it is 10 mg/kg, with a range of 7–15mg/kg. The guidelines also highlight the importance of considering body weight as a covariate for individualized anti-TB treatment.⁵

When evaluating the effectiveness of INH, the most significant predictors of treatment outcomes are the area under the concentration–time curve over a dosing interval (AUC_{0-24}) and the peak concentration (C_{max}) in relation to the minimal inhibitory concentration. These measures are especially critical for first-line TB drugs.^{6–8} In the case of INH, the target exposures are a C_{max} range of 3–6mg/L and an AUC_{0-24} of 52 mg*h/L.^{8,9} However, it is frequently observed that the actual exposure of the body to INH falls below the presumed effective range. This leads to treatment failure and the continued spread of tuberculosis.^{3,10} Due to the narrow therapeutic window of INH, accurately predicting the in vivo exposure after administration of the drug is of utmost importance in order to ensure successful treatment outcomes. To address this challenge, therapeutic drug monitoring (TDM) has emerged as a vital tool.^{8,9} TDM typically employs high-performance liquid chromatography (HPLC) or liquid chromatography-tandem mass spectrometry (LC-MS/MS) to measure INH plasma concentrations. However, fixed-time point sampling in therapeutic drug monitoring (TDM) often overlooks inter-individual variability among patients, making the accurate assessment of individual drug exposure a persistent challenge in clinical practice.

One of the key factors contributing to this inter-individual variability in INH metabolism is genetic polymorphisms in the NAT2 gene, which encodes for the N-acetyltransferase 2 enzyme involved in the metabolism of INH. The distribution frequency of NAT2 genotype and phenotype is different in different regions of the world.¹¹ In the Chinese population, the overall frequencies of NAT2 fast acetylator genotype, intermediate acetylator genotype, and slow acetylator genotype are 25.79%, 50.87%, and 23.34%, respectively. In the broader Asian population, the frequencies are 28.54% for rapid acetylators (RA), 32.47% for intermediate acetylators (IA), and 34.42% for slow acetylators (SA).^{11,12} NAT2 SA patients may experience higher drug concentrations and an increased risk of toxicity, while RA may have lower drug concentrations, potentially leading to treatment failure. These genetic differences in drug metabolism are particularly important in pediatric populations, where age-related physiological differences further complicate dosing strategies. Children are not simply smaller versions of adults, and their growing bodies undergo continuous physiological changes, including fluctuations in enzyme levels and metabolic rates that affect drug metabolism. Understanding the distribution of NAT2 phenotypes in East Asian children is crucial for developing accurate, personalized dosing regimens.¹¹ Our previous research has confirmed that INH exposure is significantly influenced by NAT2 genotypes, body weight, and other factors, with notable differences observed across ethnic groups.¹³

The PopPK approach, based on the nonlinear mixed-effects model, is a powerful tool that can be used to achieve individualized drug therapy.¹⁴ By utilizing structural, error, and covariate models, PopPK enables the definition of pharmacokinetic (PK) characteristics for a population. One notable advantage of PopPK is its ability to make use of sparsely sampled data for modeling purposes, allowing for the identification of potential covariates that contribute to intra-individual or inter-individual variability. A high-quality PopPK model is able to predict individualized exposure in vivo through the utilization of Monte Carlo simulation techniques. However, in order to ensure accurate predictions, it is crucial to employ a reasonable sampling strategy. This is where the optimal experimental design (PopED) comes into play. PopED is an optimal method that selects a specific nonlinear mixed effect model to maximize the Fisher information matrix through D-optimal design and find the optimal experimental design.¹⁵ In our study, we further optimized the sampling scheme by simulating virtual populations, estimating drug concentrations based on the proposed sampling strategy, and re-estimating model parameters from the simulated results. From these simulations, we selected the sampling strategy that provided the highest confidence in parameter estimates and minimized estimation errors,

thereby identifying the optimal sampling combination for the study. By harnessing population pharmacokinetics, this approach significantly enhances the individualized prediction capability of anti-tuberculosis therapy.¹⁶

Numerous articles have been published that discuss and review PopPK models of isoniazid, however, based on our previous work and an examination of the extant literature, no PopPK model specific to the pediatric population in China has been reported for isoniazid thus far.^{3,13,17} Currently, the recommended sampling strategy for INH in adults is to collect blood samples at 1, 2, and 6 hours after administration, as these time points have been shown to accurately reflect INH exposure. However, it is unclear whether this same sampling scheme is applicable to the pediatric population.¹⁸ To address this knowledge gap, our study aims to optimize the sampling strategy for INH in pediatric patients using the PopED technique, hoping to provide valuable insights and guidance for future pediatric clinical studies involving INH and facilitate effective monitoring of blood drug concentrations in this specific population.

Methods

Model Selection and Extraction

This article is based on the findings of previous PopPK studies of INH systematic reviews.^{13,17} Published PopPK studies were excluded if they did not give full model parameters or did not use a nonlinear mixed-effects model to analyze INH PK parameters. To better understand the pharmacokinetics of INH in the East Asian pediatric population, only PopPK models developed for East Asian adults and foreign children were included in the analysis. The PopPK models developed for adults were optimized by incorporating an allometric scaling model and extrapolating the findings to children. In allometric growth model, body weight covariates are added to relevant parameters of clearance rate and volume of distribution. The allometric amplification ratio of clearance related Parameters (CL/Q) and volume of distribution correlation coefficient is different, which is generally set as 0.75 and 1.0.

$$CL = \text{Theta}(CL) * (WT/70)^{0.75}$$

$$V = \text{Theta}(V) * (WT/70)^{1.0}$$

Two authors independently extracted the following information from eligible articles: (1) study characteristics: country, sample number, number of patients, sampling schedule, NAT2 phenotype, age, weight (WT), daily dose and limit of quantitation (LOQ); (2) PopPK characteristics: model parameters and formula, structural models, covariates, covariates involved method, inter-individual variability (IIV), inter-occasion variability (IOV), and residual unexplained variability (RUV).

Model Assumption

To account for the variability in model stability and predictive performance, we incorporated IIV into the estimation of all the main PK model parameters, including clearance, volume of distribution, and absorption constants. The IIV for all parameters was fixed at a commonly accepted value of 30%, ensuring the model's stability while maintaining clinical relevance.

In order to simulate different patient populations, we defined virtual patients representing neonates, infants, and children. The neonates had a weight of 3 kg and were 0 years old, the infants weighed 14 kg and were 2 years old, and the children weighed 28 kg and were 10 years old. Additionally, we investigated the impact of NAT2 phenotypes on the clearance of INH. These phenotypes, including SA, IA, and RA, were included in the optimization process to accurately estimate INH clearance. To determine the appropriate dosage for each virtual patient, we assigned 30, 120, and 270 mg of INH to the neonates, infants, and children, respectively. These dosages were based on the virtual typical population weight and the administration schedule recommended by the WHO. Due to the rapid absorption, distribution, and elimination of INH, there was no significant drug accumulation in the body, we only investigated the exposure after a single dose of INH in this study.

It is worth noting that some PopPK models can have a complex structure, resulting in potential overestimation of PK parameters. To address this issue and ensure accurate estimates, we employed a proper model lumping method. This

technique involves merging certain compartments of the model, thereby reducing its size and complexity.¹⁹ It can be accepted if the concentration–time curve is similar after lumping model.

Optimal Strategy

PopED package (version 0.6.0, <https://andrewhooker.github.io/PopED/>), is a D-optimal tool designed to automatically optimize experimental designs in both population and individual studies using nonlinear mixed-effect models. These models are often based on the Fisher Information Matrix (FIM), which plays a key role in optimizing the observation of a study. The Fisher Information Matrix (FIM) serves as an objective function to determine the optimal sampling scheme that maximizes the amount of information contained in the observations. By optimizing the sampling strategy based on FIM, researchers can ensure accurate estimation of parameter variance using the acquired data. Therefore, the FIM can be employed as a means to evaluate the accuracy of the parameter estimation in the sampling strategy. Ordinary differential equation (ODE) model is built using MrgSolve package (version 1.0.6, <https://mrgsolve.org/>). Regarding the composition of study cohorts, each group is stratified based on the NAT2 phenotype and weight of pediatric patients, with a total of 100 virtual patients in each group. This stratification ensures that the study encompasses a diverse range of individuals, allowing for comprehensive analysis and generalizability of the results. In order to streamline the study design and ensure feasibility, the maximum number of sampling points in all studies is limited to no more than 5. These sampling points, identified as C1 to C5, serve as reference points for data collection and enable researchers to capture relevant information while minimizing the burden on study participants.

Optimal Comparison

In our study, we conducted an analysis and comparison of different sampling schemes. Firstly, we examined adult sampling strategies that have been previously reported in the literature. These strategies involved sampling at different time intervals after administration, specifically at 1, 2, and 6 hours. Next, we employed an automated optimization approach to determine the optimal sampling strategy. This involved considering various factors, such as the model parameters and the desired accuracy of parameter estimation. The aim was to find the sampling scheme that would yield the most precise results. In addition to the optimal sampling strategy, we also explored a near-optimal sampling strategy. This strategy was developed as a secondary optimization step, based on the best results obtained from the previous optimization process. However, it also took into consideration the practical aspects of clinical operability. This means that the near-optimal strategy was designed to be more feasible and easily implementable in a clinical setting.

To assess the performance of each sampling strategy, we analyzed two key indicators: the FIM and the relative standard error (%RSE) of model parameter estimation. These metrics provided insights into the reliability and precision of the parameter estimates obtained from each strategy. The near-optimal sampling strategy could be accepted when the parameter estimation %RSE was considered acceptable and the FIM did not show a significant decrease compared to other strategies. This criterion was used to determine the suitability of the near-optimal strategy for the study. For accurate parameter estimation, the FIM value should be as large as possible. Key pharmacokinetic parameters, such as CL and V_c , should have %RSE (Relative Standard Error) estimates less than 30%, indicating precise and reliable parameter estimation.

Finally, it is essential to recognize that the final sampling strategy should be formulated by integrating all optimization results while also considering clinical feasibility. Based on the PopED optimization outcomes, we recommend determining the sampling time windows in a flexible, context-specific manner. Specifically, the selection of sampling times should be driven by clinical judgment and the particular needs of the study. This approach is intended to provide clinical researchers, including doctors and nurses, with a practical, adaptable sampling scheme that aligns with clinical practices. The final strategy, which includes these clinically tailored sampling windows, is referred to as the optimal clinical sampling strategy.

Stochastic Simulation and Estimation

To further verify the optimal clinical sampling strategy, we conduct external validation using Stochastic Simulation and Estimation (SSE), which is widely recognized as the gold standard for evaluating sampling strategies. There is no public

population database for East Asian children, we generated 100 virtual child patients using physiologically based pharmacokinetic (PBPK) modeling software PK-sim (Version 11, Bayer AG, Germany), the software has a built-in database of the physiological characteristics of the Japanese population. These virtual patients were created with a balanced male/female ratio of 1:1. To assign NAT2 phenotypes to our virtual patients, we referred to the distribution frequency (13/25/12) of NAT2 phenotypes in East Asian populations. This ensured that our simulated dataset accurately represented the variability observed in real patients. Administering the drug at 8:00 a.m., we randomly determined the sampling time for each patient within the predefined optimal clinical sampling strategy windows.

In order to appropriately assess the quality of each study, we calculated the weights based on the number of observed points and the number of patients included in each study. However, to ensure the robustness of our model, we decided to exclude models with a weight of less than 2. This meant that any models with fewer than 2 data points for a single patient were not included in SSE analysis. The SSE process involved the following steps: Firstly, we generated a series of simulated datasets (1000 times) using the included model. Next, we fitted the input model to these simulated datasets. Finally, we computed a set of statistical measures to assess the accuracy of the parameter estimates obtained from the simulated data in comparison to the true parameter values. By calculating the relative bias for these 1000 SSE results, we were able to evaluate the ability of the optimal sampling strategy to accurately estimate the model parameters. If the estimation of model parameters strategy to be acceptable, the relative bias was calculated from the following equation:

$$\text{relative bias} = 100\% \frac{1}{N} \sum_i \frac{\text{est}_i - \text{true}_i}{\text{true}_i}$$

Based on the results of 1000 SSE using the optimal clinical sampling strategy, the relative bias for key pharmacokinetic parameters should be less than 30% for the majority of studies. This ensures that the sampling strategy consistently provides accurate estimations of critical pharmacokinetic parameters, reflecting its reliability and robustness.

Results

Study Characteristics

A total of 8 studies were included in this study, with 4 focusing on adult populations and 4 focusing on pediatric populations.^{20–27} The characteristics of the PopPK models included in this study are summarized in [Table 1](#). For the adult models, studies conducted in China and South Korea were selected, while studies conducted in South Africa, Vietnam, and India were chosen for the pediatric models. All of the model data used in this analysis were prospective, and four of the studies were multi-center studies. Many of the studies used a sparse sampling strategy, meaning that only a limited number of blood samples were taken from each participant. The weight of three studies is less than 2.5, and the average sampling points of these studies are less than 2.^{21,22,26}

Population Pharmacokinetic Characteristics

The PopPK parameters estimated by the included models are presented in [Table 2](#). The most commonly used algorithm for estimating these parameters was first-order conditional estimation with the η - ϵ interaction. In most studies, the pharmacokinetics (PK) of INH were described using a two-compartment model with first-order absorption and elimination. In the pediatric PopPK models, an allometric growth model was consistently used to account for age-related changes in drug disposition. Additionally, the absorption process in the children's models was characterized using a transit model, which accounted for the time required for the drug to be absorbed into the bloodstream.^{20,24,27} To explain inter-individual variability in PK, exponential models were used in all of the included studies. The model optimization results for extrapolating from adults to children were generally consistent with those obtained from foreign pediatric populations. Some of the included models have a complex structure, involving multiple compartments and additional physiological parameters.^{24,25} After lumping models, the concentration–time performance is similar and shown in [Supplementary Figure 1](#). The lumping process was described in detail in the [Supplementary material](#).

Table I Characteristics of Included INH popPK Studies

Study (Publication Year)	Country (Type of Study)	Number of Subjects (M/F)	NAT2 Phenotype (RA/IA/SA) [%]	Number of Observations	Study Weight	Sampling Schedule	Age (Years) Mean \pm SD Median [Range]	Weight (Kg) Mean \pm SD Median [Range]	Formulation	Daily Dose Mean \pm SD Median [Range]	Bioassay [LOQ] (ng/mL)
Jing (2022) ²⁶	China(Prospective)	89(59/30)	36.0/42.7/21.3	195	2.19	0.5–6 h post-dose	44.0[16.0–72.0]	58.0[35.0–100.0]	Tablets	300/600 mg/d	LC-MS/MS [100]
Gao (2020) ²³	China (Prospective/Multi-centre)	217(147/70)	46.0/32.0/22.0	1230	5.67	Predose and 1, 2, 4, 6, 8 h post-dose	41.0 \pm 10.6	52.0 \pm 9.7	FDC tablets	225–300 mg/d	LC-MS/MS [10]
Chen (2022) ²¹	China (Prospective/Multi-centre)	202(134/68)	45.1/39.1/15.8	244	1.21	0–14 h post-dose	30.2[19.0–64.0]	61.4[39.0–78.0]	Tablets	300–900 mg/d	HPLC [120]
Cho (2021) ²²	Korea (Prospective/Multi-centre)	454(303/149)	40.5/46.7/11.7.1: unknown	477	1.05	Predose and 0–24 h post-dose	55.4 \pm 17.4	60.0 \pm 11.7	Tablets	100–400 mg/d	LC-MS/MS [100]
Zvada (2014) ²⁷	South Africa (Prospective/Multi-centre)	76(40/36)	21.0/39.0/39.05: unknown	715	9.41	Steady state	2.17[0.417–10.7]	10.5[4.90–21.8]	FDC tablets	5–10 mg/kg/d	LC-MS/MS [100] HPLC [150]
Aruldhas (2018) ²⁰	India (Prospective)	41(29/12)	31.0%/69.0	290	7.07	Predose and 0.5, 1, 1.5, 2, 2.5, 4, 6 h post-dose	7.0[3.5–13.0]	19.5[13.7–33.7]	Tablets	75–300 mg/d	LC-MS/MS [10]
Guiastrennec (2018) ^{*24}	India (Prospective)	161(91/70)	32.0%/68.0	805	5.00	Predose and 2, 4, 6, 8 h post-dose	8.0[6.0–11.0]	17.5[13.9–22.5]	Tablets	75–300 mg/d	HPLC [250]
Horita (2018) ^{*25}	Ghana (Prospective)	113(63/50)	11.0/44.0/45.0	561	4.96	Predose and 1, 2, 4, 8 h post-dose	5.0[2.17–8.25]	14.3[9.7–20.1]	FDC tablets	7–15 mg/kg/d	LC-MS/MS [97.7]

Notes: Study Weight: number of observation/ number of patients. *Lumped model: simplified model.

Abbreviations: FDC, fixed-dose combination; LOQ, limits of quantitation; HPLC, high performance liquid chromatography; LC-MS/MS, liquid chromatography tandem mass spectrometry; NAT2, N-acetyltransferase-2; SA, slow acetylator, IA, intermediate acetylator; RA, rapid acetylator.

Table 2 (Continued).

Study (Publication Year)	Software (Algorithm)	Structural Model	Fixed Effect Parameters	Between-Subject Variability (%CV) [#]	Residual Unexplained Variability Prop.err.sd (%) Add.err.sd(mg/L)
Aruldas(2018) ²⁰	NONMEM (FOCE-I)	One-compartment disposition model with a transit absorption model	MTT =0.547 NN =5 FIX Ka =(NN+1)/MTT F =1 CL =NAT2*(BW/19.4)^0.75 NAT2:SA=2.59; IA/RA=7.79 Vc =29.7*(BW/19.4)	/	0.0967 mg/L
Guiastrennec(2018) ^{*24}	NONMEM (FOCE-I)	Two-compartment with transit absorption and linear elimination	Ka =2.54 MTT =1.08 NN =8.53 CL =(4.41*1/[1+((PMA)/49)^(-2.19)]*(1+NAT2*0.944)+1.61)*(BW/17.8)^0.75 NAT2: SA=0; IA/RA=1 Vc =19.9*(BW/17.8) F =1*(1-0.195*HIV)*(1-NAT2*0.214)*(BW/17.8)^0.711 NAT2: SA=0; IA/RA=1	/	22.4%0.162 mg/L
Horita(2018) ^{*25}	Monolix (SAEM)	Two-compartment with first-order absorption and elimination	Ka =4.23 CL =(NAT2+8.46)*(BW/14.3)^0.75 NAT2:SA=4.44; IA/RA=8.08 Vc =16.6*(BW/14.3)	30	19.3%0.0393 mg/L

Notes: The unit of PK parameters: Ka (h^{-1}); CL or Q (L/h); Vc or Vp (V); MTT or Tlag (h); F (%). *Lumped model: simplified model; [#]IV of main PK parameters were assuming as 30%.

Abbreviations: Ka, absorption rate constant; CL, clearance of central compartment; Vc, distribution volume of central compartment; Q, clearance between central compartment and periphery compartment; Vp, distribution volume of periphery compartment; MTT, mean transition time; NN, number of transit compartment; F, bioavailability; Tlag, the lag time; Prop.err.sd, standard deviation of proportional residual error; Add.error.sd, standard deviation of additional residual error.

Optimal Strategy

The comparison of current and optimal and near-optimal strategies was conducted to evaluate their parameters estimation performance, and the results were summarized in [Table 3](#). Among the studies reviewed, except for two specific studies that reported high FIM under the adult sampling design,^{20,21} the remaining studies had extremely low FIM values, indicating that the current adult sampling strategy is unable to accurately estimate the parameter estimated %RSE.

To overcome these limitations, the PopED sampling design optimization was implemented, which significantly improved the parameter estimated FIM values for all models. Moreover, the %RSE values were significantly reduced, indicating a higher precision in the estimation process. Based on the findings from all included studies, it was determined that five times sampling was sufficient and yielded accurate results for the major pharmacokinetic parameters. The average %RSE values for these parameters, including CL (3.72%), Vc (23.77%), Ka (26.45%), Vp (24.48%), and Q (48.86%), were all lower than 50%. The average FIM value across all models was 3.27×10^{28} .

For the models with higher weight, the near-optimal results showed similar FIM and %RSE values compared to the optimal results. This indicated a high level of accuracy in model estimation for these cases. The average %RSE values for the main PK parameters, including CL (3.92%), Vc (5.24%), Ka (6.63%), Vp (21.02%), and Q (13.37%), were all lower than 30%. The average FIM value for these models was 2.78×10^{28} .

The near-optimal results were visually presented in [Figure 1](#). The clinical questionnaire survey was collected and the sample strategies were shown in [Supplementary material](#). However, it was recognized that sampling during lunchtime (12:00–14:00) and resting at night (22:00–6:00) might not be feasible in a clinical setting. Taking these factors into account, the final sampling strategy was determined to be collecting blood samples at 0.25 [0–0.5], 1.5 [1–2], 6 [3–8], 12 [9–14], and 24 [22–24] hours after drug administration, as these time points were considered clinically acceptable.

Stochastic Simulation and Estimation

After performing 1000 times of SSE, the results obtained for the estimation of parameter values in high-weight INH PopPK models showed a relative bias that was deemed acceptable. Specifically, the estimation of major PK parameters demonstrated a lower bias, with the value being less than 25%. The graphical representation of these results showed in [Figure 2](#).

Furthermore, the estimation %RSE of PK parameters were provided in [Table 4](#). The analysis revealed that, considering the current sampling strategy, the estimated %RSE values for the entire PK model were less than 30%. However, when estimating the clearance values for two-compartment and one-compartment models, the %RSE values were found to be significantly larger. This discrepancy can be attributed to the influence of Gao's (2020) study,²³ which suggests that uncertainties arise when extrapolating PK parameters from adults to children. Overall, the devised sampling strategy, which involved the use of sampling windows, was deemed acceptable for this study.

Discussion

This study pioneers the optimization of sampling design based on a comprehensive isoniazid population pharmacokinetic (PopPK) model repository, successfully yielding a tailored sampling strategy for INH in East Asian pediatric populations, incorporating a convenient sampling time window for enhanced practicality in clinical sample collection. Addressing the challenges posed by over-parameterized PopPK models, lumping methods have been employed to simplify the model while maintaining model accuracy, thereby enhancing the efficiency of parameter estimation. Despite physiological differences between children and adults, allometric scaling has been utilized to approximate exposure profiles, enabling effective model optimization even across these age groups.

To more effectively accommodate the disparities between adult and pediatric populations, we integrated an allometric growth model into the adult-oriented PopPK framework. This adaptation enhanced the model's predictive power, aligning it more closely with the empirical findings observed in pediatric cases. This outcome substantiated the feasibility of extrapolating from adult to pediatric populations under these circumstances. In conjunction with the application of the allometric growth model, the researchers meticulously examined the influence of covariates in both adult and pediatric models. It was revealed that postmenstrual age (PMA), NAT2 phenotype, and body weight played a principal role in

Table 3 Comparison of Optimal Sampling Strategy

Study	Population		Former Design	FIM	Optimal Design	FIM	Evaluation		Near Optimal Design	FIM	Evaluation	
	Items	Value					Parameters	%RSE			Parameters	%RSE
Jing (2022) ²⁶	NAT2 (Phenotype) BW (kg) Dose (mg)	SA 3 30	1, 2, 9	1.80E-26	0.00001, 0.4122, 3.082, 12, 23.76	2.14E+21	CL	3.89	0.1, 0.5, 3, 12, 24	4.29E+15	CL	4.86
		Vc	26.54	Vc	61.27							
	Ka	28.74	Ka	76.59								
	Q	53.19	Q	149.11								
	Vp	10.6	Vp	18.53								
	NAT2 (Phenotype) BW (kg) Dose (mg)	SA 14 120	1, 2, 9	4.32E-24	1.001e-05, 0.3958, 1.329, 4.326, 24	2.43E+17	CL	3.37	0.1, 0.4, 1.5, 4, 24	3.92E+16	CL	3.35
		Vc	48.12	Vc	53.5							
	Ka	48.25	Ka	55.34								
Q	44.02	Q	53.33									
Vp	20.7	Vp	22.46									
NAT2 (Phenotype) BW (kg) Dose (mg)	SA 28 240	1, 2, 9	-1.11E-22	1.001e-05, 0.5265, 2.837, 12, 24	1.44E+16	CL	3.46	0.1, 0.5, 3, 12, 24	4.19E+14	CL	3.85	
	Vc	162.38	Vc	545.58								
Ka	162.48	Ka	549.6									
Q	107.06	Q	360.09									
Vp	78.28	Vp	257.42									
NAT2 (Phenotype) BW (kg) Dose (mg)	IA 3 30	1, 2, 9	-1.78E-19	0.0004428, 0.8041, 4, 11.79, 23.76	5.49E+25	CL	4.02	0.1, 1, 4, 12, 24	6.56E+19	CL	3.78	
	Vc	14.55	Vc	7.18								
Ka	14.12	Ka	10.98									
Q	0.19	Q	49.74									
Vp	7.45	Vp	21.33									
NAT2 (Phenotype) BW (kg) Dose (mg)	IA 14 120	1, 2, 9	-4.73E-19	0.08563, 0.6571, 3.388, 12, 24	1.50E+23	CL	3.56	0.1, 0.5, 4, 12, 24	9.62E+20	CL	3.21	
	Vc	6.85	Vc	21.81								
Ka	6.59	Ka	20.03									
Q	11.1	Q	23.89									
Vp	5.59	Vp	4.98									
NAT2 (Phenotype) BW (kg) Dose (mg)	IA 28 240	1, 2, 9	3.18E-19	0.03674, 0.5918, 2.837, 12, 21.22	1.86E+20	CL	3.45	0.1, 0.5, 3, 12, 24	1.74E+16	CL	4.32	
	Vc	13.19	Vc	218.73								
Ka	14.27	Ka	220.65									
Q	25.32	Q	249.79									
Vp	5.53	Vp	6.22									
NAT2 (Phenotype) BW (kg) Dose (mg)	RA 3 30	1, 2, 9	8.30E-19	0.001284, 0.4122, 4, 11.18, 21.31	1.39E+22	CL	3.81	0.1, 0.5, 4, 12, 24	2.38E+20	CL	4.38	
	Vc	5.41	Vc	6.58								
Ka	3.49	Ka	21.39									
Q	6.74	Q	91.78									
Vp	6.03	Vp	37.75									

Gao (2020) ²³	NAT2 (Phenotype) BW (kg) Dose (mg)	RA 14 120	1, 2, 9	-3.26E-18	0.0179, 0.4939, 3.694, 12, 21.06	2.95E+27	CL Vc Ka Q Vp	3.78 13.63 12.59 16.91 0.0071	0.1, 0.5, 4, 12, 24	1.85E+24	CL Vc Ka Q Vp	3.72 12.37 9.43 7.61 4.01
	NAT2 (Phenotype) BW (kg) Dose (mg)	RA 28 240	1, 2, 9	-2.46E-19	0.04797, 0.6245, 3.449, 12, 23.97	1.01E+20	CL Vc Ka Q Vp	3.56 18.64 17.02 19.58 3.03	0.1, 0.5, 3, 12, 24	1.58E+19	CL Vc Ka Q Vp	3.52 14.29 13.26 19.71 5.93
	NAT2 (Phenotype) BW (kg) Dose (mg)	SA 3 30	1, 2, 9	6.11E-11	0.2, 1, 3.309, 7.136, 21.42	8.00E+24	CL Vc Ka Q Vp	4.33 5.33 4.93 6.06 13.14	0.2, 1, 3, 8, 24	6.45E+24	CL Vc Ka Q Vp	4.36 5.17 4.75 5.77 13.58
	NAT2 (Phenotype) BW (kg) Dose (mg)	SA 14 120	1, 2, 9	3.18E-12	0.2, 1, 4, 8.18, 24	3.15E+24	CL Vc Ka Q Vp	4.75 5.94 5.36 5.89 15.2	0.2, 1, 4, 8, 24	3.14E+24	CL Vc Ka Q Vp	4.75 5.99 5.4 5.94 15.15
	NAT2 (Phenotype) BW (kg) Dose (mg)	SA 28 240	1, 2, 9	-5.45E-12	0.2, 1, 4, 8.41, 24	1.88E+24	CL Vc Ka Q Vp	4.94 6.95 6.24 5.91 16.21	0.2, 1, 4, 8, 24	1.83E+24	CL Vc Ka Q Vp	4.93 7.11 6.4 5.95 16.21
	NAT2 (Phenotype) BW (kg) Dose (mg)	IA 3 30	1, 2, 9	-3.03E-12	0.2, 1, 3.165, 6.787, 19.89	6.69E+23	CL Vc Ka Q Vp	4.69 5.57 5.19 7.98 18.61	0.2, 1, 3, 6, 24	5.04E+23	CL Vc Ka Q Vp	4.99 5.66 5.24 9.24 19.3
	NAT2 (Phenotype) BW (kg) Dose (mg)	IA 14 120	1, 2, 9	-4.39E-13	0.2, 1, 3.939, 7.942, 24	4.45E+23	CL Vc Ka Q Vp	5.14 5.64 5.14 7.94 20.88	0.2, 1, 4, 8, 24	4.45E+23	CL Vc Ka Q Vp	5.15 5.66 5.17 7.94 20.91

(Continued)

Table 3 (Continued).

Study	Population		Former Design	FIM	Optimal Design	FIM	Evaluation		Near Optimal Design	FIM	Evaluation	
	Items	Value					Parameters	%RSE			Parameters	%RSE
Chen (2022) ²¹	NAT2 (Phenotype) BW (kg) Dose (mg)	IA 28 240	1, 2, 9	-1.55E-12	0.2, 1, 4, 8.245, 24	4.12E+23	CL	5.27	0.2, 1, 4, 8, 24	4.07E+23	CL	5.26
		Vc	5.97	Vc	6.03							
		Ka	5.36	Ka	5.42							
		Q	7.84	Q	7.89							
		Vp	21.69	Vp	21.61							
	NAT2 (Phenotype) BW (kg) Dose (mg)	RA 3 30	1, 2, 9	2.27E-18	0.1674, 0.9163, 2.876, 5.945, 17	5.36E+19	CL	6.46	0.2, 1, 3, 6, 24	3.22E+19	CL	7.76
		Vc	7.32	Vc	7.58							
		Ka	6.81	Ka	6.98							
		Q	21.38	Q	25.27							
		Vp	53.57	Vp	64.82							
NAT2 (Phenotype) BW (kg) Dose (mg)	RA 14 120	1, 2, 9	-6.22E-17	0.2, 1, 3.49, 7.03, 22.29	9.43E+19	CL	7.22	0.2, 1, 3.5, 8, 24	8.15E+19	CL	7.24	
	Vc	6.1	Vc	5.98								
	Ka	5.65	Ka	5.54								
	Q	22.11	Q	21.41								
	Vp	59.12	Vp	60.26								
NAT2 (Phenotype) BW (kg) Dose (mg)	RA 28 240	1, 2, 9	-5.31E-16	0.2, 1, 3.816, 7.592, 24	1.90E+20	CL	7.2	0.2, 1, 4, 8, 24	1.85E+20	CL	7.21	
	Vc	5.66	Vc	5.79								
	Ka	5.24	Ka	5.39								
	Q	21.62	Q	21.32								
	Vp	58.35	Vp	58.9								
NAT2 (Phenotype) BW (kg) Dose (mg)	SA 3 30	1, 2, 9	2.84E+08	1.001e-05, 1.001e- 05, 1.76, 1.774, 24	2.17E+15	CL	3.62	0.1, 2, 24	3.73E+13	CL	4.12	
	Vc	3.79	Vc	4.41								
	Ka	4.36	Ka	6.14								
	Q	3.6	Q	4.08								
	Vp	3.83	Vp	4.5								
NAT2 (Phenotype) BW (kg) Dose (mg)	SA 14 120	1, 2, 9	6.76E+07	1.001e-05, 1.001e- 05, 1.728, 1.728, 24	1.98E+15	CL	3.6	0.1, 2, 24	3.41E+13	CL	4.08	
	Vc	3.83	Vc	4.5								
	Ka	4.43	Ka	6.32								
	Q	3.6	Q	4.06								
	Vp	3.84	Vp	4.52								
NAT2 (Phenotype) BW (kg) Dose (mg)	SA 28 240	1, 2, 9	4.10E+07	1.001e-05, 1.755, 1.959, 23.51	4.40E+14	CL	3.6	0.1, 2, 24	3.23E+13	CL	4.06	
	Vc	3.84	Vc	4.52								
	Ka	4.99	Ka	6.36								
	Q	3.96	Q	3.98								
	Vp	4.28	Vp	3.41								
NAT2 (Phenotype) BW (kg) Dose (mg)	IA 3 30	1, 2, 9	4.53E+09	0.09919, 0.2, 1.98, 12, 23.76	5.64E+14	CL	3.96	0.1, 2, 12, 24	2.75E+14	CL	3.98	
	Vc	4.28	Vc	3.41								
	Ka	5.63	Ka	5.94								

Cho (2021) ²²	NAT2 (Phenotype) BW (kg) Dose (mg)	IA 14 120	1, 2, 9	6.00E+08	1.423e-05, 0.2, 1.857, 4, 24	6.06E+14	CL Vc Ka	3.7 3.87 5.48	0.1, 2, 4, 24	2.44E+14	CL Vc Ka	3.66 3.81 5.45
	NAT2 (Phenotype) BW (kg) Dose (mg)	IA 28 240	1, 2, 9	2.73E+08	1e-05, 1.758, 24	7.57E+13	CL Vc Ka	4.15 4.44 5.38	0.1, 2, 24	3.74E+13	CL Vc Ka	4.11 4.41 6.16
	NAT2 (Phenotype) BW (kg) Dose (mg)	RA 3 30	1, 2, 9	1.41E+11	1e-05, 0.2, 1.918, 21.06	3.68E+18	CL Vc Ka	3.53 0.47 5.26	0.1, 2, 24	3.42E+15	CL Vc Ka	3.57 1.3 7.41
	NAT2 (Phenotype) BW (kg) Dose (mg)	RA 14 120	1, 2, 9	1.19E+10	0.1537, 1.857, 12, 23.51	2.49E+14	CL Vc Ka	2.98 3.49 6.11	0.2, 2, 12, 24	8.84E+13	CL Vc Ka	3.94 4.12 6.19
	NAT2 (Phenotype) BW (kg) Dose (mg)	RA 28 240	1, 2, 9	4.32E+09	0.04083, 0.2, 1.735, 12, 23.27	7.12E+16	CL Vc Ka	3.25 1.34 4.34	0.1, 2, 12, 24	9.35E+16	CL Vc Ka	2.69 1.47 5.39
	NAT2 (Phenotype) BW (kg) Dose (mg)	SA 3 30	1, 2, 9	-1.26E-33	0.05012, 0.677, 2.351, 6.122, 16.18	7.26E+20	CL Vc Ka Q Vp	3.45 135.2 134.69 114.93 11.92	0.1, 0.5, 2, 8, 24	4.99E+18	CL Vc Ka Q Vp	3.53 356.31 355.25 315.11 38.1
	NAT2 (Phenotype) BW (kg) Dose (mg)	SA 14 120	1, 2, 9	2.08E-33	0.05913, 0.9023, 2.754, 7.07, 22.65	7.24E+21	CL Vc Ka Q Vp	3.48 42.71 42.01 20.55 10.53	0.1, 1, 3, 8, 24	5.09E+21	CL Vc Ka Q Vp	3.48 52.02 50.99 24.25 12.79
	NAT2 (Phenotype) BW (kg) Dose (mg)	SA 28 240	1, 2, 9	1.22E-33	0.06183, 1, 2.966, 8.359, 24	7.78E+21	CL Vc Ka Q Vp	3.43 38.46 37.7 13.26 11.13	0.1, 1, 3, 8, 24	6.89E+21	CL Vc Ka Q Vp	3.43 38.98 37.93 13.17 11.18
	NAT2 (Phenotype) BW (kg) Dose (mg)	IA 3 30	1, 2, 9	7.06E-34	0.05008, 0.6003, 2.45, 6.111, 12	3.30E+20	CL Vc Ka Q Vp	3.6 215.97 215.51 282.54 66.39	0.1, 0.5, 3, 6, 12	1.06E+20	CL Vc Ka Q Vp	4.38 251.95 250.75 327.77 80.48

(Continued)

Table 3 (Continued).

Study	Population		Former Design	FIM	Optimal Design	FIM	Evaluation		Near Optimal Design	FIM	Evaluation	
	Items	Value					Parameters	%RSE			Parameters	%RSE
Zvada (2014) ²⁷	NAT2 (Phenotype) BW (kg) Dose (mg)	IA 14 120	1, 2, 9	1.71E-32	0.05738, 0.8472, 2.703, 5.862, 12.2	2.36E+22	CL Vc Ka Q Vp	3.46 32.17 31.49 27.09 5.74	0.1, 1, 3, 6, 12	1.57E+22	CL Vc Ka Q Vp	3.45 38.31 37.22 30.33 5.73
	NAT2 (Phenotype) BW (kg) Dose (mg)	IA 28 240	1, 2, 9	-3.83E-32	0.05995, 0.9608, 2.933, 6.458, 14.25	3.78E+22	CL Vc Ka Q Vp	3.45 26.84 26.11 17.7 5.94	0.1, 1, 3, 6, 12	1.90E+22	CL Vc Ka Q Vp	3.42 28.66 27.62 18.13 5.79
	NAT2 (Phenotype) BW (kg) Dose (mg)	RA 3 30	1, 2, 9	1.05E-33	0.05078, 0.5503, 2.329, 5.833, 12	4.46E+19	CL Vc Ka Q Vp	3.89 431.8 431.1 708.81 257.34	0.1, 1, 3, 6, 12	7.36E+18	CL Vc Ka Q Vp	3.55 611.92 604.28 948 351.66
	NAT2 (Phenotype) BW (kg) Dose (mg)	RA 14 120	1, 2, 9	2.15E-32	0.05605, 0.803, 2.644, 5.521, 12	1.06E+22	CL Vc Ka Q Vp	3.58 33.4 32.79 38.16 8.15	0.1, 1, 3, 6, 12	6.09E+21	CL Vc Ka Q Vp	3.55 44.53 43.3 47.51 9.33
	NAT2 (Phenotype) BW (kg) Dose (mg)	RA 28 240	1, 2, 9	-2.09E-34	0.05867, 0.9185, 2.82, 5.79, 12	4.59E+22	CL Vc Ka Q Vp	3.5 23.41 22.67 21.02 6.24	0.1, 1, 3, 6, 12	3.55E+22	CL Vc Ka Q Vp	3.5 26.27 25.25 22.76 6.23
	NAT2 (Phenotype) BW (kg) Dose (mg)	SA 3 30	1, 2, 9	2.35E-14	1.001e-05, 1, 2.643, 7.515, 24	9.57E+25	CL Vc Ka Q Vp	3.19 10.21 10.86 34.05 19.64	0.1, 1, 3, 8, 24	7.33E+25	CL Vc Ka Q Vp	3.18 9.74 10.63 32.21 18.3
	NAT2 (Phenotype) BW (kg) Dose (mg)	SA 14 120	1, 2, 9	-1.67E-15	1.001e-05, 1, 3.406, 9.642, 24	1.75E+28	CL Vc Ka Q Vp	3.21 6.33 7.09 14.69 9.52	0.1, 1, 3, 9, 24	1.35E+28	CL Vc Ka Q Vp	3.2 6.94 7.92 17.1 11.18

NAT2 (Phenotype) BW (kg)Dose (mg)	SA28240	1, 2, 9	9.17E-17	1e-05, 1, 3.751, 10.5, 24	2.09E+28	CL Vc Ka Q Vp	3.22 5.8 6.57 13.2 8.34	0.1, 1, 3, 9, 24	1.25E+28	CL Vc Ka Q Vp	3.2 6.64 7.62 17.92 11.04
NAT2 (Phenotype) BW (kg) Dose (mg)	IA 3 30	1, 2, 9	-5.99E-15	1.001e-05, 1, 2.789, 7.875, 24	8.06E+27	CL Vc Ka Q Vp	3.2 8.76 9.47 20.36 13.99	0.1, 1, 3, 8, 24	6.67E+27	CL Vc Ka Q Vp	3.21 8.59 9.52 19.8 13.48
NAT2 (Phenotype) BW (kg) Dose (mg)	IA 14 120	1, 2, 9	-2.88E-12	1e-05, 1, 3.352, 9.197, 24	3.21E+29	CL Vc Ka Q Vp	3.28 5.96 6.74 7.15 5.63	0.1, 1, 3, 9, 24	2.60E+29	CL Vc Ka Q Vp	3.25 6.49 7.47 7.73 6.2
NAT2 (Phenotype) BW (kg) Dose (mg)	IA 28 240	1, 2, 9	-1.19E-12	1.001e-05, 1, 3.692, 9.943, 24	4.52E+29	CL Vc Ka Q Vp	3.31 5.47 6.25 6.56 5.12	0.1, 1, 3, 9, 24	3.14E+29	CL Vc Ka Q Vp	3.24 6.23 7.22 7.8 6.18
NAT2 (Phenotype) BW (kg) Dose (mg)	RA 3 30	1, 2, 9	2.92E-13	1.001e-05, 1, 2.779, 7.988, 24	2.61E+28	CL Vc Ka Q Vp	3.21 8.46 9.18 16.2 11.89	0.1, 1, 3, 9, 24	2.04E+28	CL Vc Ka Q Vp	3.23 8.18 9.12 15.4 11.2
NAT2 (Phenotype) BW (kg) Dose (mg)	RA 14 120	1, 2, 9	-7.73E-11	1.001e-05, 1, 3.378, 8.596, 24	4.75E+29	CL Vc Ka Q Vp	3.33 5.97 6.76 6.02 4.97	0.1, 1, 3, 9, 24	3.73E+29	CL Vc Ka Q Vp	3.28 6.52 7.52 6.1 5.11
NAT2 (Phenotype) BW (kg) Dose (mg)	RA 28 240	1, 2, 9	-1.81E-11	1.001e-05, 1, 3.68, 9.264, 24	7.13E+29	CL Vc Ka Q Vp	3.35 5.46 6.25 5.71 4.7	0.1, 1, 3, 9, 24	5.01E+29	CL Vc Ka Q Vp	3.27 6.22 7.21 5.91 4.95

(Continued)

Table 3 (Continued).

Study	Population		Former Design	FIM	Optimal Design	FIM	Evaluation		Near Optimal Design	FIM	Evaluation	
	Items	Value					Parameters	%RSE			Parameters	%RSE
Aruldas (2018) ²⁰	NAT2 (Phenotype) BW (kg) Dose (mg)	SA330	1, 2, 9	4.68E+17	0.592, 1.421, 8.817, 8.817, 8.817	1.34E+24	CL Vc MTT*	3.01 3.01 3	0.5, 1.5, 9	7.85E+18	CL Vc MTT	3.03 3.01 3.01
	NAT2 (Phenotype) BW (kg) Dose (mg)	SA 14 120	1, 2, 9	5.08E+17	0.5922, 1.504, 12.25, 12.25, 12.3	1.33E+24	CL Vc MTT*	3.01 3.01 3.01	0.5, 1.5, 12	8.52E+18	CL Vc MTT	3.04 3.01 3.01
	NAT2 (Phenotype) BW (kg) Dose (mg)	SA 28 240	1, 2, 9	6.25E+17	0.07259, 0.4898, 1.959, 12.73, 17.3	1.46E+24	CL Vc MTT*	3.02 2.85 3.01	0.1, 0.5, 2, 12, 24	1.33E+24	CL Vc MTT	3.01 2.99 3.01
	NAT2 (Phenotype) BW (kg) Dose (mg)	USA 3 30	1, 2, 9	4.35E+17	0.5858, 1.234, 1.237, 3.821, 3.821	1.33E+24	CL Vc MTT*	3.01 3.01 3.01	0.5, 1, 4	3.96E+19	CL Vc MTT	3.03 3.01 3.01
	NAT2 (Phenotype) BW (kg) Dose (mg)	USA 14 120	1, 2, 9	6.66E+17	0.5809, 1.305, 5.097, 5.101, 5.101	1.32E+24	CL Vc MTT*	3.01 3.01 3.01	0.5, 1, 5	5.46E+19	CL Vc MTT	3.04 3.02 3.01
	NAT2 (Phenotype) BW (kg) Dose (mg)	USA 28 240	1, 2, 9	5.37E+17	0.5847, 1.338, 5.762, 5.864, 5.876	1.32E+24	CL Vc MTT*	3.01 3.01 3.01	0.5, 1.5, 6	3.82E+19	CL Vc MTT	3.04 3.01 3.01

Guiastrennec# (2018) ²⁴	NAT2 (Phenotype)	SA 3 30	1, 2, 9	-5.14E-39	1.239, 3.362, 3.362, 12.29, 12.29	3.16E+21	CL	3.56	1, 3, 12	2.78E+18	CL	4.06
	BW (kg) Dose (mg)						Vc	3.69			Vc	4.23
							Ka	6.65			Ka	8.32
	NAT2 (Phenotype)	SA14120	1, 2, 9	-6.03E-39	1.061, 3.201, 3.201, 8.981, 16.21	2.26E+22	CL	3.32	1, 3, 9, 24	2.47E+21	CL	3.49
	BW (kg)Dose (mg)						Vc	3.68			Vc	4.13
Horita (2018) # ²⁵							Ka	5.58			Ka	6.3
	NAT2 (Phenotype)	SA28240	1, 2, 9	-3.89E-42	0.5624, 0.9772, 3.334, 3.334, 10.63	4.50E+22	CL	3.28	0.5, 1, 3, 12	4.70E+21	CL	3.52
	BW (kg)Dose (mg)						Vc	3.59			Vc	3.96
							Ka	5.16			Ka	5.86
	NAT2 (Phenotype)	USA 3 30	1, 2, 9	4.14E-42	1.287, 2.837, 2.837, 6.961, 6.961	5.43E+20	CL	3.67	1, 3, 6	8.92E+17	CL	4.05
						Vc	4.25			Vc	5.56	
						Ka	8.03			Ka	10.46	
NAT2 (Phenotype)	USA 14 120	1, 2, 9	5.03E-42	1.113, 2.772, 2.772, 6.295, 6.295	7.43E+21	CL	3.34	1, 3, 6	4.20E+19	CL	3.54	
BW (kg) Dose (mg)						Vc	4.06			Vc	5.07	
						Ka	6.27			Ka	7.36	
NAT2 (Phenotype)	USA 28 240	1, 2, 9	-2.58E-41	1.026, 2.948, 2.948, 7.426, 7.426	2.11E+22	CL	3.29	1, 3, 8	1.36E+20	CL	3.58	
BW (kg) Dose (mg)						Vc	3.79			Vc	4.61	
						Ka	5.48			Ka	6.47	
NAT2 (Phenotype)	SA 3 30	1, 2, 9	5.35E-41	0.02322, 1.039, 1.039, 3.669, 17.63	3.85E+27	CL	3.19	0.1, 1, 4, 24	2.64E+26	CL	3.34	
BW (kg) Dose (mg)						Vc	3.47			Vc	3.76	
						Ka	3.96			Ka	4.57	
NAT2 (Phenotype)	SA 14 120	1, 2, 9	-1.93E-43	0.0255, 1.152, 1.152, 4.938, 24	4.16E+27	CL	3.2	0.1, 1, 5, 24	3.00E+26	CL	3.35	
BW (kg) Dose (mg)						Vc	3.42			Vc	3.72	
						Ka	3.93			Ka	4.61	
NAT2 (Phenotype)	SA 28 240	1, 2, 9	-4.95E-44	0.06842, 1.267, 1.297, 5.388, 17.14	3.61E+27	CL	3.2	0.1, 1, 6, 24	3.05E+26	CL	3.36	
BW (kg) Dose (mg)						Vc	3.44			Vc	3.69	
						Ka	4.05			Ka	4.61	
NAT2 (Phenotype)	USA 3 30	1, 2, 9	4.04E-37	0.02337, 0.9545, 0.9546, 2.996, 6.857	3.24E+27	CL	3.19	0.1, 1, 3, 8	2.52E+26	CL	3.31	
BW (kg) Dose (mg)						Vc	3.55			Vc	3.89	
						Ka	4.04			Ka	4.67	
NAT2 (Phenotype)	USA 14 120	1, 2, 9	-3.22E-39	0.02565, 1.068, 1.068, 3.989, 22.04	3.84E+27	CL	3.19	0.1, 1, 4, 24	2.86E+26	CL	3.33	
BW (kg) Dose (mg)						Vc	3.46			Vc	3.76	
						Ka	3.96			Ka	4.61	
NAT2 (Phenotype)	USA 28 240	1, 2, 9	-3.03E-39	0.01682, 0.9863, 1.138, 4.677, 22.53	3.90E+27	CL	3.2	0.1, 1, 5, 24	2.88E+26	CL	3.36	
BW (kg) Dose (mg)						Vc	3.42			Vc	3.71	
						Ka	3.97			Ka	4.59	

Notes: *This study assuming: $K_a = KTR = (NN+1)/MTT$; #Lumped model: simplified model.

Abbreviations: CL, clearance of central compartment; Vc, distribution volume of central compartment; Q, clearance between central compartment and periphery compartment; Vp, distribution volume of periphery compartment; MTT, mean transition time; NAT2, N-acetyltransferase-2; SA, slow acetylator; IA, intermediate acetylator; RA, rapid acetylator.



Figure 1 Optimal sampling times of isoniazid popPK model. Point: near-optimal sampling strategy. **(A)** adult models; **(B)**, pediatric models. NAT2 phenotype. **Abbreviations:** SA, slow acetylators; IA, intermediate acetylators; RA, rapid acetylators.

governing the clearance rate of INH. Of these factors, PMA had the most profound impact on infants and neonates, with its effect diminishing progressively as age advanced. The similarity observed between the sampling optimization outcomes derived from extrapolating adult models to pediatrics and those obtained directly from optimizing pediatric models serves as evidence supporting the feasibility of applying adult-derived parameters to inform the pediatric population in the context of isoniazid pharmacokinetics.

Recently, TDM of anti-tuberculous drugs has been implemented in specialized centers.^{9,28} However, the current recommendations for dosage adjustments of INH may not be optimal, as they solely focus on achieving a 2-hour post-dose concentration between 3 and 6 mg/L. This approach overlooks the considerable IIV in the absorption and disposition kinetics of INH. Relying solely on the 2-hour post-dose concentration may not accurately estimate drug exposure, especially for narrow therapeutic index (NTI) drugs. The misestimation of the C_{max} may have serious consequences, such as an increased risk of treatment failure for individuals with rapid acetylators phenotypes and a higher likelihood of hepatotoxicity for slow acetylators.²⁹ Our approach, using a PopPK model repository, optimizes the sampling time points, ensuring that fewer plasma samples are required while still providing accurate estimations of key pharmacokinetic parameters, such as clearance and volume of distribution. This more efficient strategy reduces the complexity and invasiveness of sampling in pediatric populations without compromising model accuracy.

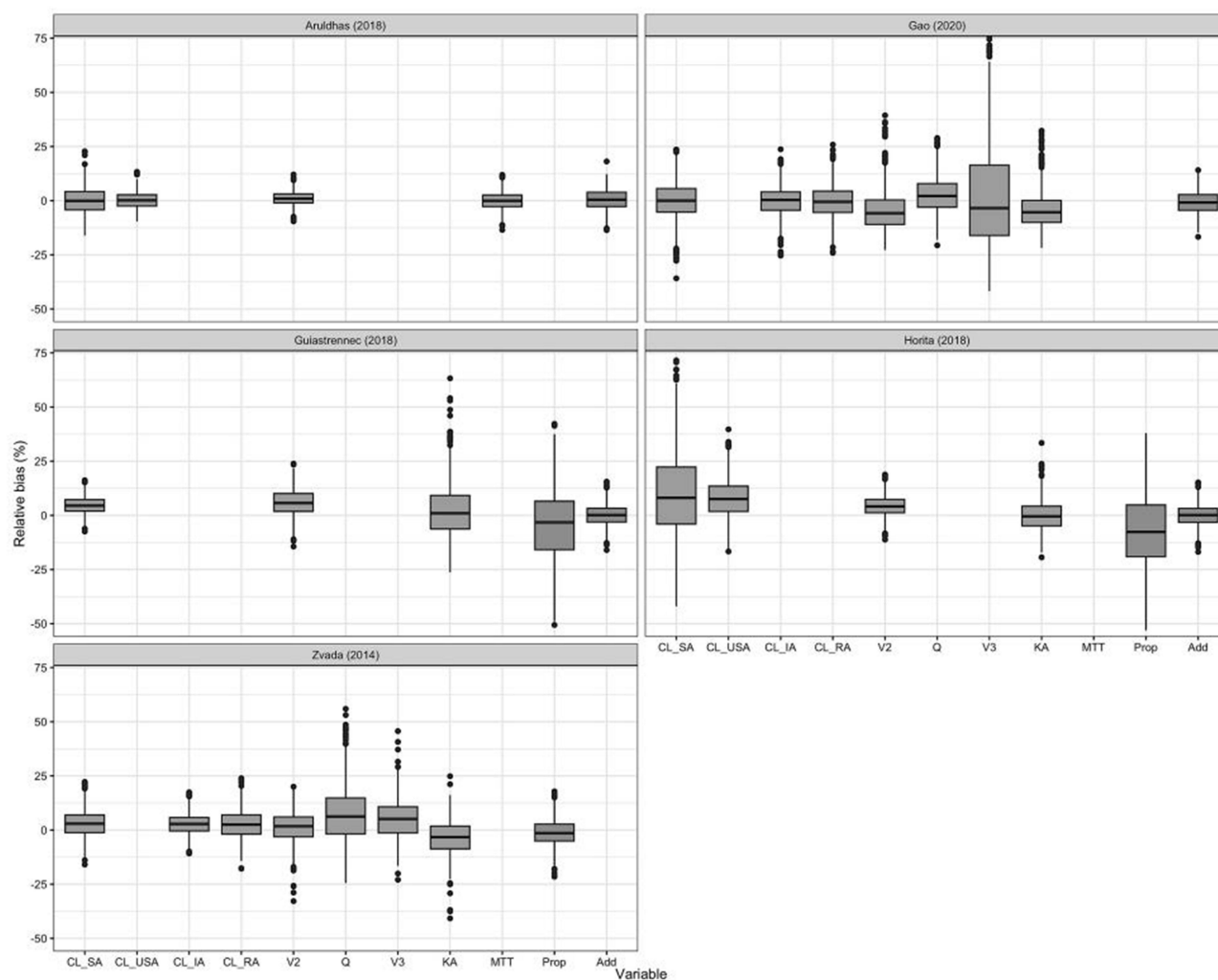


Figure 2 Relative bias % of popPK parameters estimation.

Notes: Black dot: discrete values; Box line: upper quartile, lower quartile and median value; Variable including: CL_SA: NAT2 slow acetylators clearance; CL_USA: non NAT2 slow acetylators clearance; CL_IA: NAT2 intermediate acetylators clearance; CL_RA: NAT2 rapid acetylators clearance; CL: apparent clearance; (Q) the intercompartment clearance; Vc: the apparent central compartment distribution volumes; Vp: the apparent peripheral compartment distribution volumes; Ka: absorption rate; MTT: mean transit absorption time; Prop: proportional residual error; Add: additive residual error. The more concentrated the box is towards 0, the smaller the relative bias.

It is important to note that children's pharmacokinetics differ significantly from adults, including a shorter time to peak concentration. In children, the time to reach peak concentration (T_{max}) is typically earlier than in adults. This means that existing sampling strategies—such as the widely used 1, 2, and 6 hours post-dose—are inadequate for pediatric populations.²⁹ These fixed-time sampling strategies fail to adequately capture the drug's absorption and distribution processes in children, as they cannot account for the earlier T_{max} and the different pharmacokinetic characteristics of this population. Therefore, optimizing sampling strategies for children is essential to ensure more accurate measurement of INH exposure and improve treatment outcomes.

Most of retrieved studies were focused on a single population for modeling or validation, without considering inter-group differences and cross-validation.^{18,30} In our study, we found that the recommended sampling strategy from previous studies failed to accurately estimate all child model parameters, resulting in an extremely low FIM value and an inability to estimate %RSE. To overcome these problems, we optimized the sampling strategy based on PopED and fully considered clinical operation convenience. After adding specific sampling windows, we are able to accurately estimate the main pharmacokinetic parameters in most of the INH models. The simulation and estimation results from the

Table 4 Relative Standard Error of SSE Results

Study	Subgroup	Parameters						
		CL	Vc	Ka/MTT	Q	Vp	Prop.err.sd	Add.err.sd
Guiastrennec (2018)* ²⁴ Zvada (2014) ²⁷	/	12.33	19.11	38.24	NA	NA	50.9	15.3
	NAT2_SA	19.8	22.1	28.1	25.4	39.5	2.8E-12	NA
	NAT2_IA NAT2_RA	14.7 20.7						
Aruldas (2018) ²⁰	NAT2_SA	19.08	9.95	12.73	NA	NA	NA	15.15
	NAT2_IA/RA	11.78						
Horita (2018)* ²⁵	NAT2_SA	61.09	14.21	21.37	NA	NA	54.6	15.71
	NAT2_IA/RA	27.32						
Gao (2020) ²³	NAT2_SA	26.30	28.28	26.48	25.54	104.21	16.38	88.97
	NAT2_IA	21.17						
	NAT2_RA	23.79						
Average		23.46	18.73	25.38	25.47	71.86	30.47	33.78

Note: *Lumped model; simplified model.

Abbreviations: NAT2, N-acetyltransferase-2; SA, slow acetylator; IA, intermediate acetylator; RA, rapid acetylator; Prop.err.sd, standard deviation of proportional residual error; Add.error.sd, standard deviation of additional residual error; NA, no answer.

SSE showed that the final sampling strategy, using no more than 5 plasma concentrations, provided accurate and precise estimation of INH PK parameters.

PopPK model typically simplify the complex in vivo processes of drug disposition by partitioning them into interconnected compartments. The inter-compartmental distribution processes can be mathematically represented using ordinary differential equations. The more precise the description of the drug's in vivo handling, the higher the complexity of both the system of equations and the model itself, which inherently introduces increased computational complexity.³¹ Within the repository of INH PopPK models, some exhibit issues of overparameterization, potentially leading to model overfitting and thereby complicating model estimates. In such cases, lumping methods are employed to reduce overfitting by consolidating compartments and generating new compartmental and distribution parameters through matrix operations on the parameter space. This method facilitates practical application by simplifying overly complex models. In this study, the lumping approach was applied to streamline the model into a one-compartment model, significantly enhancing the efficiency of sampling optimization strategies. It is essential to consider the necessity of model refinement, and for scenarios where transfer rates between peripheral compartments are extremely rapid or the volume of distribution is minuscule, model simplification proves feasible. Lumping techniques have been previously utilized and are widely applied in the simplification of compartmental structures within physiological pharmacokinetic models, as evidenced in earlier literature.^{32,33}

Additionally, while most previous studies have focused on sampling strategies for adults or single pediatric cohorts, our study integrates a more flexible strategy applicable to a broad range of pediatric patients, considering both physiological and pharmacokinetic variations. By optimizing the sampling windows, we significantly improve the precision of pharmacokinetic parameter estimation, ensuring more reliable dosing recommendations, particularly for children with diverse metabolic profiles, such as rapid and slow acetylators.

It is important to acknowledge the limitations of this study. This study has several limitations. First, parameter estimation was challenging for some models due to overparameterization, particularly in pediatrics. While lumping methods improved estimation, they may have missed some pharmacokinetic details. Future studies with larger datasets could help improve accuracy. Second, allometric scaling may not fully capture the physiological differences between adults and children, especially for drugs with variable pharmacokinetics. Third, the sample size was limited, and a more diverse cohort would improve generalizability. Including more covariates like genetics and comorbidities would also strengthen the findings. Lastly, the sampling strategy was designed for East Asian children, and its applicability to other populations needs further validation. This study's methodology, however, has the potential to be generalized to other pediatric populations, particularly in regions with high pediatric TB prevalence and varying genetic profiles.

Conclusion

This study demonstrates that the optimized sampling strategy for isoniazid (INH) developed for East Asian pediatric populations offers a more accurate representation of the pharmacokinetic (PK) characteristics specific to this group. This strategy, which is based on factors such as NAT2 phenotype, age, and body weight, ensures that PK estimates reflect the unique drug disposition in East Asian children. This approach is also highly applicable to drugs with strong pharmacokinetic-pharmacodynamic (PKPD) correlations and narrow therapeutic windows, similar to INH. Accurate estimation of pharmacokinetic parameters is crucial for precision dosing in high-burden countries such as China and Africa, where personalized treatment can significantly improve treatment outcomes. Given that tuberculosis treatment often involves multiple drug regimens, further research is necessary to optimize sampling strategies for other anti-tuberculosis drugs, as well as to identify the best sampling strategy that aligns with the therapeutic windows of INH and other anti-TB drugs, thereby enhancing the overall treatment regimen for tuberculosis.

Acknowledgments

Thanks to Changsha Duxact Clinical Laboratory Co., Ltd. and Phamark Data Technology Co., Ltd., Changsha, Hunan, China, for the statistical support. We used the Large Language Model-ChatGPT-in the drafting of this paper for grammar and language refinement.

Funding

The research was funded by the National Natural Science Foundation of China (No.82073942); Hunan Key Laboratory for Bioanalysis of Complex Matrix Samples (2017TP1037); The science and technology innovation Program of Hunan Province (2023RC3232); Hunan Science and Technology Youth Talent Support Program (2023TJ-N20); Hunan Innovation platform and talent program (2020RC3086).

Disclosure

There are no competing interests to declare.

References

1. Organization WH. Global tuberculosis report. 2022 [cited March 07, 2023]; Available from: <https://www.who.int/publications-detail-redirect/9789240061729>. Accessed April 17, 2025.
2. Peloquin CA, Davies GR. The treatment of tuberculosis. *Clin Pharmacol Ther.* 2021;110(6):1455–1466. doi:10.1002/cpt.2261
3. Alsultan A, Peloquin CA. Therapeutic drug monitoring in the treatment of tuberculosis: an update. *Drugs.* 2014;74(8):839–854. doi:10.1007/s40265-014-0222-8
4. Erwin ER, Addison AP, John SF, et al. Pharmacokinetics of isoniazid: the good, the bad, and the alternatives. *Tuberculosis.* 2019;116s:S66–s70. doi:10.1016/j.tube.2019.04.012
5. Organization, W.H. WHO consolidated guidelines on tuberculosis: tuberculosis preventive treatment: module 1: prevention [Internet]. 2020 [cited 2023 March 07]; Available from: <https://www.who.int/publications/i/item/9789240001503>. Accessed April 17, 2025.
6. Gumbo T, Louie A, Liu W, et al. Isoniazid bactericidal activity and resistance emergence: integrating pharmacodynamics and pharmacogenomics to predict efficacy in different ethnic populations. *Antimicrob Agents Chemother.* 2007;51(7):2329–2336. doi:10.1128/AAC.00185-07
7. Jayaram R, Shandil RK, Gaonkar S, et al. Isoniazid pharmacokinetics-pharmacodynamics in an aerosol infection model of tuberculosis. *Antimicrob Agents Chemother.* 2004;48(8):2951–2957. doi:10.1128/AAC.48.8.2951-2957.2004
8. Pasipanodya JG, McIlleron H, Burger A, et al. Serum drug concentrations predictive of pulmonary tuberculosis outcomes. *J Infect Dis.* 2013;208(9):1464–1473. doi:10.1093/infdis/jit352
9. Martson AG, Burch G, Ghimire S, et al. Therapeutic drug monitoring in patients with tuberculosis and concurrent medical problems. *Expert Opin Drug Metab Toxicol.* 2021;17(1):23–39. doi:10.1080/17425255.2021.1836158
10. Azuma J, Ohno M, Kubota R, et al. NAT2 genotype guided regimen reduces isoniazid-induced liver injury and early treatment failure in the 6-month four-drug standard treatment of tuberculosis: a randomized controlled trial for pharmacogenetics-based therapy. *Eur J Clin Pharmacol.* 2013;69(5):1091–1101. doi:10.1007/s00228-012-1429-9
11. Surarak T, Chumnumwat S, Nosoongnoen W, et al. Efficacy, safety, and pharmacokinetics of isoniazid affected by NAT2 polymorphisms in patients with tuberculosis: a systematic review. *Clin Transl Sci.* 2024;17(4):e13795. doi:10.1111/cts.13795
12. Wang Ning ZL-Y, Xiu-juan M. Distribution characteristics of N-acetyltransferase-2 genotypes and comparison methods of different genotyping in Chinese population. *Chin J Antituberculosis.* 2022;44(6):625–634.
13. Ju G, Liu X, Yang W, et al. Model-informed precision dosing of isoniazid: parametric population pharmacokinetics model repository. *Drug Des Devel Ther.* 2024;18:801–818. doi:10.2147/DDDT.S434919
14. Ludden TM. Population pharmacokinetics. *J Clin Pharmacol.* 1988;28(12):1059–1063. doi:10.1002/j.1552-4604.1988.tb05714.x

15. Nyberg J, Bazzoli C, Ogungbenro K, et al. Methods and software tools for design evaluation in population pharmacokinetics-pharmacodynamics studies. *Br J Clin Pharmacol*. 2015;79(1):6–17. doi:10.1111/bcp.12352
16. Sturkenboom MGG, Mårtson A-G, Svensson EM, et al. Population pharmacokinetics and bayesian dose adjustment to advance TDM of Anti-TB drugs. *Clin Pharmacokinet*. 2021;60(6):685–710. doi:10.1007/s40262-021-00997-0
17. Li J, Cai X, Chen Y, et al. Parametric population pharmacokinetics of isoniazid: a systematic review. *Expert Rev Clin Pharmacol*. 2023;16(5):467–489. doi:10.1080/17512433.2023.2196401
18. Cojutti P, Giangreco M, Isola M, et al. Limited sampling strategies for determining the area under the plasma concentration–time curve for isoniazid might be a valuable approach for optimizing treatment in adult patients with tuberculosis. *Int J Antimicrob Agents*. 2017;50(1):23–28. doi:10.1016/j.ijantimicag.2017.01.036
19. Yau E, Olivares-Morales A, Ogungbenro K, et al. Investigation of simplified physiologically-based pharmacokinetic models in rat and human. *CPT Pharmacometrics Syst Pharmacol*. 2023;12(3):333–345. doi:10.1002/psp4.12911
20. Aruldhas BW, Hoglund RM, Ranjalkar J, et al. Optimization of dosing regimens of isoniazid and rifampicin in children with tuberculosis in India. *Br J Clin Pharmacol*. 2019;85(3):644–654. doi:10.1111/bcp.13846
21. Chen B, Shi H-Q, Feng MR, et al. Population pharmacokinetics and pharmacodynamics of isoniazid and its metabolite acetylisoniazid in Chinese population. *Front Pharmacol*. 2022;13:932686. doi:10.3389/fphar.2022.932686
22. Cho YS, Jang TW, Kim H-J, et al. Isoniazid population pharmacokinetics and dose recommendation for Korean patients with tuberculosis based on target attainment analysis. *J Clin Pharmacol*. 2021;61(12):1567–1578. doi:10.1002/jcph.1931
23. Gao Y, Davies Forsman L, Ren W, et al. Drug exposure of first-line anti-tuberculosis drugs in China: a prospective pharmacological cohort study. *Br J Clin Pharmacol*. 2021;87(3):1347–1358. doi:10.1111/bcp.14522
24. Guaiastrenec B, Ramachandran G, Karlsson MO, et al. Suboptimal antituberculosis drug concentrations and outcomes in small and HIV-coinfected children in India: recommendations for dose modifications. *Clin Pharmacol Ther*. 2018;104(4):733–741. doi:10.1002/cpt.987
25. Horita Y, Alsultan A, Kwarra A, et al. Evaluation of the adequacy of WHO revised dosages of the first-line antituberculosis drugs in children with tuberculosis using population pharmacokinetic modeling and simulations. *Antimicrob Agents Chemother*. 2018;62(9). doi:10.1128/AAC.00008-18.
26. Jing W, Zong Z, Tang B, et al. Population pharmacokinetic analysis of isoniazid among pulmonary tuberculosis patients from China. *Antimicrob Agents Chemother*. 2020;64(3). doi:10.1128/AAC.01736-19.
27. Zvada SP, Denti P, Donald PR, et al. Population pharmacokinetics of rifampicin, pyrazinamide and isoniazid in children with tuberculosis: in silico evaluation of currently recommended doses. *J Antimicrob Chemother*. 2014;69(5):1339–1349. doi:10.1093/jac/dkt524
28. Heysell SK, Moore JL, Staley D, et al. Early therapeutic drug monitoring for isoniazid and rifampin among diabetics with newly diagnosed tuberculosis in Virginia, USA. *Tuberc Res Treat*. 2013;2013:129723. doi:10.1155/2013/129723
29. Pasipanodya JG, Srivastava S, Gumbo T. Meta-analysis of clinical studies supports the pharmacokinetic variability hypothesis for acquired drug resistance and failure of antituberculosis therapy. *Clin Infect Dis*. 2012;55(2):169–177. doi:10.1093/cid/cis353
30. Magis-Escurra C, Later-Nijland HMJ, Alffenaar JWC, et al. Population pharmacokinetics and limited sampling strategy for first-line tuberculosis drugs and moxifloxacin. *Int J Antimicrob Agents*. 2014;44(3):229–234. doi:10.1016/j.ijantimicag.2014.04.019
31. Brochot C, Tóth J, Bois FY. Lumping in pharmacokinetics. *J Pharmacokinet Pharmacodyn*. 2005;32(5–6):719–736. doi:10.1007/s10928-005-0054-y
32. Aarons LJ, Arundel PA, Rowland M, Nestorov IA. Lumping of whole-body physiologically based pharmacokinetic models. *J Pharmacokinet Biopharm*. 1998;26(1):21–46. doi:10.1023/A:1023272707390
33. Ryu HJ, Kang W-H, Kim T, et al. A compatibility evaluation between the physiologically based pharmacokinetic (PBPK) model and the compartmental PK model using the lumping method with real cases. *Front Pharmacol*. 2022;13:964049. doi:10.3389/fphar.2022.964049

Drug Design, Development and Therapy

Publish your work in this journal

Drug Design, Development and Therapy is an international, peer-reviewed open-access journal that spans the spectrum of drug design and development through to clinical applications. Clinical outcomes, patient safety, and programs for the development and effective, safe, and sustained use of medicines are a feature of the journal, which has also been accepted for indexing on PubMed Central. The manuscript management system is completely online and includes a very quick and fair peer-review system, which is all easy to use. Visit <http://www.dovepress.com/testimonials.php> to read real quotes from published authors.

Submit your manuscript here: <https://www.dovepress.com/drug-design-development-and-therapy-journal>

Dovepress
Taylor & Francis Group